Top quark forward-backward asymmetry in the little Higgs model *

GUO Xing-Dao(郭星导)[1] ZHANG Yin-Jie(张印杰)[1] ZHAO Shu-Min(赵树民)[1;1)]
FENG Tai-Fu(冯太傅)[1;2)] YUAN Xu-Hao(袁煦浩)[2] LI Xue-Qian(李学潜)[3]

[1] Department of Physics and Technology, Hebei University, Baoding 071002, China
[2] Center for High Energy Physics, Department of Engineering Physics, Tsinghua University, Beijing 100084, China
[3] Department of Physics, Nankai University, Tianjin 300071, China

Abstract: A sizable difference in top quark pair forward backward asymmetry (AFB) is observed at Tevatron. The discrepancy triggers many new physics beyond the standard model (SM) and then constrains the parameter spaces in them. In this article we calculate the AFB of the top-pair production at Tevatron up to next to leading order (NLO) in the little Higgs model (LHM). We find that the contribution of Z_H can be large enough to make up the gap between SM prediction and experimental data. Then, the parameter space for the couplings between Z_H and quarks are constrained. Thus, this model can fulfill the experimental data, both in AFB and in cross section.

Key words: forward-backward asymmetry, little Higgs model, one-loop diagram, Feynman amplitude

PACS: 11.30.Er, 12.60.Jv **DOI:** 10.1088/1674-1137/38/11/113102

1 Introduction

In recent years, the top quark pair production and its decays have been investigated theoretically and experimentally [1–3]. Although the theoretical predictions for the total cross section of top quark pair production [4–6] are in agreement with the experimental results [7, 8], the top quark forward-backward asymmetry (AFB) between theoretical predictions and experimental data are in discrepancy. The AFB in the $t\bar{t}$ rest frame is defined as

$$A_{\rm FB}\equiv\frac{N_{\rm t}(y_{\rm t}-y_{\bar{\rm t}}>0)-N_{\rm t}(y_{\rm t}-y_{\bar{\rm t}}<0)}{N_{\rm t}(y_{\rm t}-y_{\bar{\rm t}}>0)+N_{\rm t}(y_{\rm t}-y_{\bar{\rm t}}<0)}, \tag{1}$$

where $\Delta y=y_{\rm t}-y_{\bar{\rm t}}$ is the difference of the rapidities of outgoing t and $\bar{\rm t}$. The difference of the rapidities of outgoing t and $\bar{\rm t}$ is directly related to θ as [9]

$$\Delta y=y_{\rm t}-y_{\bar{\rm t}}=2{\rm arctanh}\left(\sqrt{1-\frac{4m_{\rm t}^2}{\hat{s}}}\cos\theta\right), \tag{2}$$

where $\hat{s}=(p_{\rm t}+p_{\bar{\rm t}})^2$, θ is the angle spanned between the outgoing top quark and incoming proton beam, and the rapidity is defined as

$$y_{\rm t}=\frac{1}{2}\ln\left[\frac{E_{\rm t}+p_{\rm t\|}}{E_{\rm t}-p_{\rm t\|}}\right], \tag{3}$$

where $E_{\rm t}$ and $p_{\rm t\|}$ stand for the energy and longitudinal component of the momentum of the top quark, respectively. The sign of $\Delta y=y_{\rm t}-y_{\bar{\rm t}}$ is the same as $\cos\theta$, so that the asymmetry in Eq. (1) can be re-defined as

$$A_{\rm FB}=\frac{N_{\rm t}(\cos\theta>0)-N_{\rm t}(\cos\theta<0)}{N_{\rm t}(\cos\theta>0)+N_{\rm t}(\cos\theta<0)}. \tag{4}$$

The measurements of the CDF and D0 Collaborations yield $A_{\rm FB}=0.158\pm0.075$ [10], $A_{\rm FB}=0.162\pm0.047$ [11] and $A_{\rm FB}=0.196\pm0.065$ [12], and the central values are significantly larger than the Standard Model (SM) prediction, $A_{\rm FB}^{\rm SM}=0.089$ [13]. This discrepancy has motivated people to consider additional contributions from new physics beyond SM (BSM) [14, 15].

In some models, an exchange of new particles of color-octet at the s-channel contributes [16–18]. Instead, a color singlet particle that mediates the interaction may also provide a substantial contribution through the t-channel if it has both vector and axial vector coupling to $q\bar{q}$ and $t\bar{t}$ [9]. This kind of model receives severe constraints from the data of the $t\bar{t}$ production rate. However, as one notices, a color singlet particle can also make a substantial contribution to the AFB through s-channel

Received 28 February 2014, Revised 3 June 2014

∗ Supported by National Natural Science Foundation of China (10975027, 11275036, 11047002), Natural Science Foundation of Hebei Province (A2013201277 , A2011201118) Natural Science Fund of Hebei University (2011JQ05, 2007113), open project of State Key Laboratory of Mathematics-Mechanization (Y3KF311CJ1) and Natural Science Fund of Hebei University (2011JQ05, 2012-242)

1) E-mail: zhaosm@mail.hbu.edu.cn

2) E-mail: fengtf@dlut.edu.cn

resonance. The little Higgs model (LHM) is just one such model.

The LHM can solve the hierarchy problem of particle physics, and therefore is a favorable extension of the SM. The LHM begins with an $SU(5)$ global symmetry, which is spontaneously broken down to its subgroup $SO(5)$ via a non-zero vacuum expectation value f, leaving 14 Goldstone bosons that transform under the electroweak gauge group as a real singlet 1_0, a real triplet 3_0, a complex doublet $2_{\pm\frac{1}{2}}$, and a complex triplet $3_{\pm1}$. The real singlet and the triplet become the longitudinal components of the gauge bosons associated with the broken gauge groups, giving them masses of the order f. These gauge bosons are $\mathrm{w_L^{\pm}}$, $\mathrm{A_L}$, $\mathrm{Z_L}$, $\mathrm{w_H^{\pm}}$, $\mathrm{A_H}$ and $\mathrm{Z_H}$. Among them, $\mathrm{w_H^{\pm}}$, $\mathrm{A_H}$ and $\mathrm{Z_H}$ are new particles in the LHM.

In this work we calculate the AFB in the LHM in $\mathrm{t\bar{t}}$ rest frame and, by comparing the theoretical prediction with the data, we set constraints on the model parameters. We find that there exists a possible parameter space for the LHM, with which the AFB reported by the CDF and D0 collaborations [19] can be well explained.

This paper is organized as follows. After this introduction, in Sections 2 and 3, we derive the theoretical formulas for the cross section of the top-pair production up to next to leading order in the LHM. In Section 4, a detailed analysis on the asymmetry is presented. Then, the numerical results along with all the input parameters are outlined. The last section is devoted to a discussion and our conclusion.

2 Contribution of leading-order diagram to the asymmetry

The LHM consists of four new bosons, but only $\mathrm{A_H}$ and $\mathrm{Z_H}$, whose masses are, respectively, $m_{\mathrm{A_H}} \propto f g_{\mathrm{vu}}$ and $m_{\mathrm{Z_H}} \propto f\left(g'_{\mathrm{vu}}+\dfrac{1}{g'_{\mathrm{vu}}}\right)$, can contribute asymmetry through s-channel with couplings

$$\begin{aligned}\mathcal{L}_{\mathrm{A_H}} &= A_{\mathrm{H}}\bar{t}(g_{\mathrm{vt}}+g_{\mathrm{at}}\gamma^5)\gamma^\mu t \\ &\quad +A_{\mathrm{H}}\bar{u}(g_{\mathrm{vu}}+g_{\mathrm{au}}\gamma^5)\gamma^\mu u, \end{aligned} \tag{5}$$

and

$$\begin{aligned}\mathcal{L}_{\mathrm{Z_H}} &= Z_{\mathrm{H}}\bar{t}(g'_{vt}+g'_{at}\gamma^5)\gamma^\mu t \\ &\quad +Z_{\mathrm{H}}\bar{u}(g'_{\mathrm{vu}}+g'_{au}\gamma^5)\gamma^\mu u. \end{aligned} \tag{6}$$

The relations among the coupling constants are listed in the appendix of Ref. [20] and their numerical values are presented in Section 4. An $A_{\mathrm{FB}}^{\mathrm{t}}$, which may be consistent with the Tevatron data, can be generated in $\mathrm{q\bar{q}}\to\mathrm{t\bar{t}}$ within this model. In order to formulate the whole contribution to the forward backward asymmetry for top quark from LHM, we compute the tree diagrams analytically and calculate the corresponding box diagrams numerically. The leading-order diagrams are shown in Fig. 1.

The amplitude of the first diagram of Fig. 1 can be written as:

$$\mathcal{M}_{1a}=\bar{u}(p_4)(-i\gamma^\mu g_{\mathrm{s}})v(p_3)\frac{-\mathrm{i}}{(p_1+p_2)^2}\bar{v}(p_2)(-\mathrm{i}\gamma_\mu g_{\mathrm{s}})u(p_1), \tag{7}$$

where p_1 and p_2, respectively, stand for the four-momenta of the initial state ($\mathrm{q\bar{q}}$), and p_3, p_4 denote the four-momenta of the final state ($\mathrm{t\bar{t}}$). $p_1+p_2=p_3+p_4$ stands for the energy-momentum conservation. For the other two diagrams, the amplitudes are similar, so we skip them. The contributions at tree level are shown above, and the numerical results will be given in section 4.

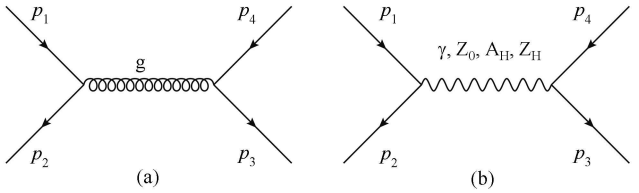

Fig. 1. The tree diagrams for the process of $\mathrm{q\bar{q}}\to\mathrm{t\bar{t}}$.

3 Next-to-leading-order diagrams in LHM

In this section, we calculate the next to leading order contribution to the forward-backward asymmetry. The box diagrams contributing to the asymmetry are shown as Fig. 2.

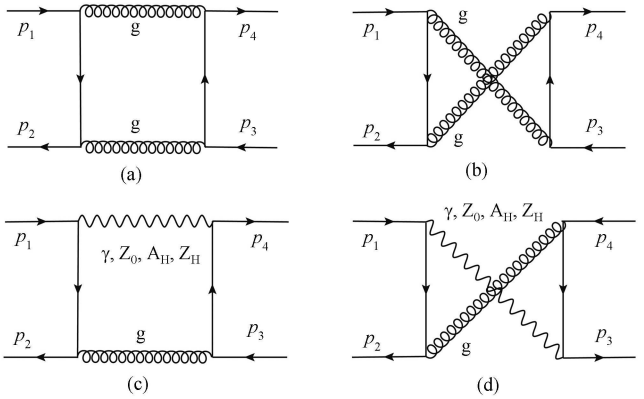

Fig. 2. The box diagrams for the process of $\mathrm{q\bar{q}}\to\mathrm{t\bar{t}}$.

The diagrams for real-gluon emission are presented in Fig. 3 and Fig. 4.

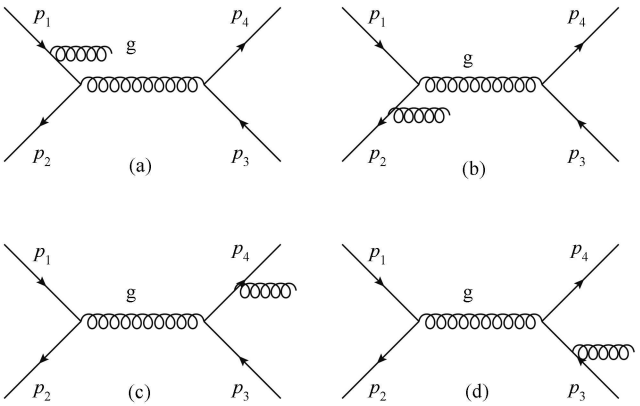

Fig. 3. The real-gluon emission diagrams for the process of $q\bar{q} \to t\bar{t}+g$ with gluon being the intermediate boson at s-channel. In (a) and (b) the real gluon is emitted from the initial state while in (c) and (d) it is emitted from one of the produced top quarks.

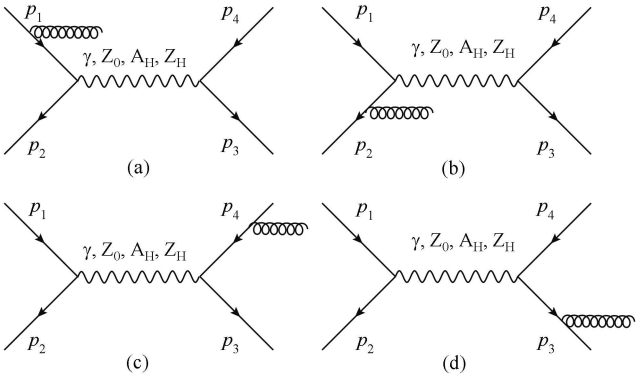

Fig. 4. The real-gluon emission diagrams for the process of $q\bar{q}\to t\bar{t}+g$ with A_H or Z_H being the intermediate boson at s-channel. In (a) and (b) the real gluon is emitted from the initial state while in (c) and (d) it is emitted from one of the produced top quarks.

The amplitude of the first diagram in the Fig. 2 is:

$$\begin{aligned}\mathcal{M}_{2a} &= \int\frac{\mathrm{d}^4k}{(2\pi)^4}\bar{u}(p_4)\frac{-\mathrm{i}}{q^2}(-\mathrm{i}g_s\gamma^\mu T^b_{ij})\frac{\mathrm{i}(\not{p}_4+\not{q}+m_4)}{(p_4+q)^2-m_4^2}\\ &\times(-\mathrm{i}g_s\gamma^\nu T^a_{jk})v(p_3)\bar{v}(p_2)(-\mathrm{i}g_s\gamma^\nu T^a_{mn})\\ &\times\frac{-\mathrm{i}}{(p_1+p_2+q)^2}(-\mathrm{i}g_s\gamma^\mu T^b_{nl})\frac{\mathrm{i}(\not{p}_1+\not{q}+m_2)}{(p_1+q)^2-m_2^2}u(p_1). \quad (8)\end{aligned}$$

For the other diagrams, the amplitudes are similar but the coupling vertices are different. The box diagrams have infrared divergences that can be canceled by adding the real-gluon emission diagrams (Fig. 3 and Fig. 4), and we take into account the interference between initial and final state gluon emission. The dependence of the resultant differential cross section on $\cos\theta$ is:

$$\begin{aligned}\frac{\mathrm{d}\hat{\sigma}}{\mathrm{d}\cos\theta} &= \frac{2\pi\sqrt{1-\frac{4m_t^2}{\hat{s}}}}{64\pi^2\hat{s}}\frac{1}{4}\sum|\mathcal{M}_1+\mathcal{M}_2|^2\\ &= \frac{\sqrt{1-\frac{4m_t^2}{\hat{s}}}}{128\pi\hat{s}}\sum(|\mathcal{M}_1|^2+2\mathrm{Re}(\mathcal{M}_1^*\mathcal{M}_2)), \quad (9)\end{aligned}$$

where $\hat{s}=zxs$ and z x stand for the longitudinal fraction of $q/\bar{q}$ in proton/anti-proton separately. We can then obtain the theoretical prediction on the cross section, which has been measured for the process by convoluting the sub-processes with the parton distribution functions of proton and anti-proton.

$$\frac{\mathrm{d}\sigma_{tot}}{\mathrm{d}\cos\theta}=\int_0^1\mathrm{d}x\int_0^1\mathrm{d}z f(x)f(z)\frac{\mathrm{d}\hat{\sigma}}{\mathrm{d}\cos\theta}. \quad (10)$$

The total differential cross section Eq. (10) involves $f(x)$ and $f(z)$, which are the parton distribution functions (PDF) of proton and anti-proton, respectively. Here, we adopt the parton distribution function from CTEQ6M [21]. The asymmetry is determined by integrating over the positive and negative range of the $\cos\theta$. The numerical results are presented in section 4.

4 Numerical results

In this section, we calculate the differential cross section numerically. We set the mass of top quark as 175 GeV and neglect the mass of light quarks. With the weak-binding approximation, that is $p_q=p_{\bar{q}}$ and $p_q^2=m_q^2$, we get

$$\begin{aligned}p_1.p_2 &= \frac{\hat{s}}{2}, p_3.p_4=\frac{\hat{s}}{2}-m_t^2,\\ p_1.p_3 &= p_2.p_4=\frac{\hat{s}}{4}\left(1+\sqrt{1-\frac{4m_t^2}{\hat{s}}}\cos\theta\right), \quad (11)\\ p_1.p_4 &= p_2.p_3=\frac{\hat{s}}{4}\left(1-\sqrt{1-\frac{4m_t^2}{\hat{s}}}\cos\theta\right).\end{aligned}$$

The input parameters that we are going to use in the numerical computations are set as follows [20, 22–24]: $\alpha_s=0.104$ for $\mu=m_t$. In the LHM [20], we choose

$$g_{vu}=-0.0292\left(\frac{3}{a}-2a\right);\ g_{au}=-0.0175\left(\frac{3}{a}-2a\right);$$

$$g_{vd}=0.2742\frac{3}{a}+0.245a;\ \ g_{ad}=0.0175\left(\frac{3}{a}-2a\right);$$

$$g_{vt}=-0.0292\left(\frac{3}{a}-2a\right)-0.35\left(\frac{1}{a}+a\right)b;$$

$$g_{\rm at}=-0.0175\left(\frac{3}{a}-2a\right)-0.35\left(\frac{1}{a}+a\right)b;$$

$$g_{\rm ve}=0.0525\left(\frac{3}{a}-2a\right);g_{\rm ae}=0.0175\left(\frac{3}{a}-2a\right);$$

and $m_{A_{\rm H}}=0.08138\left(\frac{1}{a}+a\right)f$ GeV [20]; where a and b are the parameters in Ref. [20] and we let them vary from 0.1 to 2 and 0 to 1, respectively. For the $Z_{\rm H}$ boson, $m_{Z_{\rm H}}=0.0539\left(36.73g'_u+\frac{1}{g'_u}\right)f$ GeV, and for simplicity we use the relation $g'_{\rm vu}=-g'_{\rm vd}=g'_{\rm vt}=-g_{\rm ve}=-g'_{\rm au}=g'_{\rm ad}=-g'_{\rm at}=g'_{\rm ae}=0.165a$. These could vary from 0.0165 to 0.33 [20], and the coupling constant $\alpha_{\rm l}=\frac{g'^2_{\rm au}}{4\pi}$, which varies from 0.00002 to 0.00867. In the following calculation, we take $f=500$, 1000, 1500 GeV, respectively.

One important constraint is the total production cross section of the $t\bar{t}$ pair measured in recent experiment. The averaged value for $t\bar{t}$-production cross section at Tevatron is $\sigma^{\rm exp}(t\bar{t})=7.65\pm0.20\pm0.36$ pb [25]. Considering the experimental data from Ref. [7, 8], we believe that taking the experimental value of the $t\bar{t}$ cross section to be 7.1–8.2 pb is reasonable. The SM prediction on the top quark cross section is 6.7 pb [4], which coincides with our numerical result and is 20% larger than 5.6 pb [13](only LO result). In Ref. [13, 26], the QED correction to asymmetry is about 20%, but the weak correction is only 10^{-5} [13]. In this article the same result is also taken.

After calculation, we find that the $A_{\rm H}$ boson contribution is so small that we can neglect it safely, thus $Z_{\rm H}$ offers the main contribution. The coupling constant of Weak interaction and that of the interaction between quarks and $Z_{\rm H}$ are of the same order of magnitude, so in NLO their contributions should be same, both are about 10^{-5} [13]. However, in LO the contribution from $Z_{\rm H}$ is larger than that from weak interaction for the resonance.

The uncertainties come from the PDF, $m_{\rm t}$, $\alpha_{\rm s}(\mu)$, $m_{Z_{\rm H}}$ and the coupling constants between $Z_{\rm H}$ and quarks. From Ref. [26] we can get that the PDF and $m_{\rm t}$ have a small effect on asymmetry. However, the varying $\alpha_{\rm s}(\mu)$ obviously changes the cross section and asymmetry [13, 26]. In Ref. [4] the cross section varies from 7.10 pb to 5.96 pb when μ varies from $\frac{m_{\rm t}}{2}$ to $2m_{\rm t}$. So, after calculating the uncertainty range of total cross section in, our result is ±0.4 pb. In Ref. [13] the asymmetry varies from 9.7% to 8.3% when μ varies in the same region. After calculation, the uncertainty range of asymmetry is $\pm0.3\%$. For the two cuts $M_{t\bar{t}}>450$ GeV and $|\Delta y|>1$, the uncertainty ranges are $\pm2\%$ and $\pm3\%$ separately. Lastly, $m_{Z_{\rm H}}$ and the coupling constants between $Z_{\rm H}$ and quarks are varying with the parameter a mentioned above. In following we will show how this parameter can be limited by experimental data.

We demonstrate the dependence of the total cross section on the coupling constant in Fig. 5, and the dependence of AFB on the coupling constant in Fig. 6.

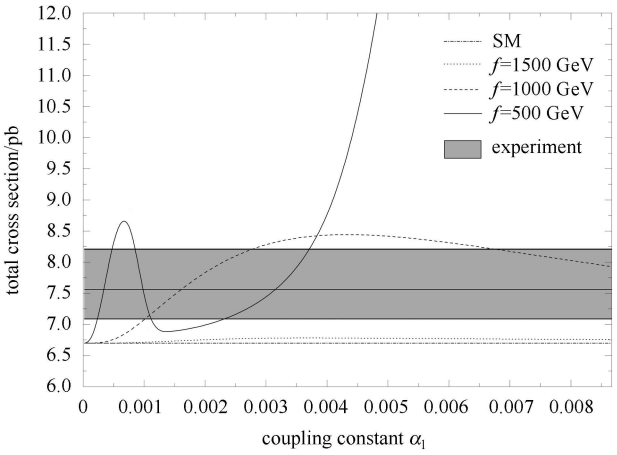

Fig. 5. The dependence of the total cross section on the coupling constant in the frameworks of SM and LHM with $f=500$ GeV (solid), $f=1000$ GeV (dashed), $f=1500$ GeV (dotted) respectively. The dash-dotted line stands for the value from SM [4], and the shadowed region is for experimental data with errors [25]. The uncertainty range is ±0.4 pb for μ in $\alpha_{\rm s}(\mu)$ varies from $\frac{m_{\rm t}}{2}$ to $2m_{\rm t}$.

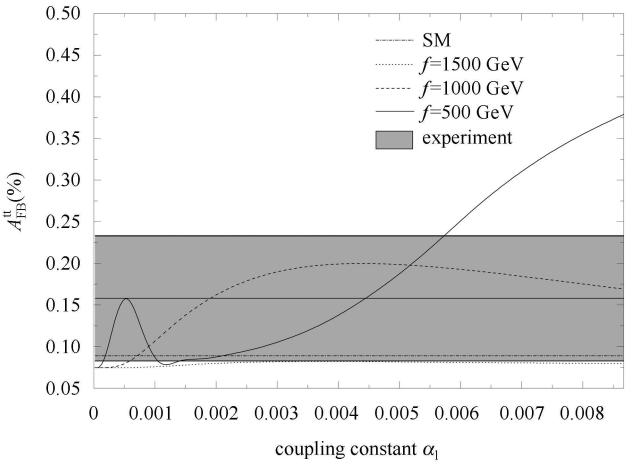

Fig. 6. The AFB versus coupling constant in the frameworks of SM and LHM with $f=500$ GeV (solid), $f=1000$ GeV (dashed), $f=1500$ GeV (dotted). The dash-dotted line stands for the value from SM [4], and the shadowed region is for experimental data with errors [10]. The uncertainty range is $\pm0.3\%$ for μ in $\alpha_{\rm s}(\mu)$ varies from $\frac{m_{\rm t}}{2}$ to $2m_{\rm t}$.

From Fig. 5 we can see that for $f=500$ GeV, when taking the coupling constant as 0.0002–0.0005, 0.0008–0.0012 and 0.0023–0.0037, the theoretical predictions on

the total cross section are inside the experimental tolerance range. While for $f=1000$ GeV, the theoretical prediction does not conflict with the experimental data when the coupling constant is about 0.0010–0.0028 and 0.0067–0.0087. As for $f=1500$ GeV, one can scarcely find a region that can match the experimental data.

In Fig. 6 we find that for $f=500$ GeV, when taking the coupling constant below 0.0057, the AFB almost matches the experimental data. For $f=1000$ GeV, the theoretical prediction fits the experimental value when the coupling constant is above 0.0006. But it is hard to find an area that can match the experimental data with $f=1500$ GeV.

We also analyze our results for taking two different kinds of cuts. One is for $t\bar{t}$ $M_{t\bar{t}}>450$ GeV and the other is for rapidity $|\Delta y|>1$. These results are shown in Fig. 7 and Fig. 8.

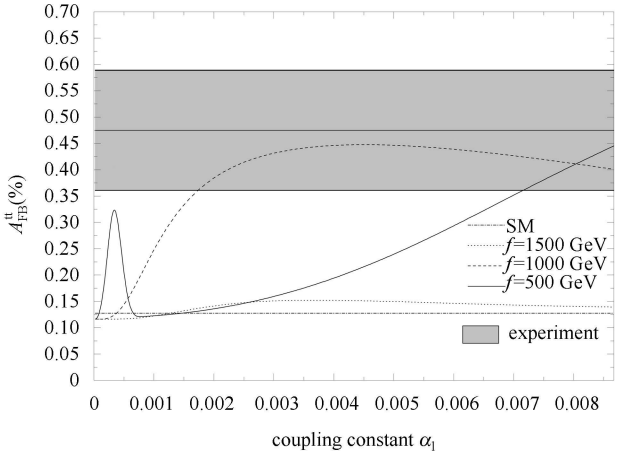

Fig. 7. The AFB with a cut of $M_{t\bar{t}}>450$ GeV versus the coupling constant in the frameworks of SM and LHM with $f=500$ GeV (solid), $f=1000$ GeV (dashed), $f=1500$ GeV (dotted). The dash-dotted line stands for the value from SM [13], and the shadowed region is for the experimental data [10]. The uncertainty range is $\pm 2\%$ for μ in $\alpha_s(\mu)$ varies from $\frac{m_t}{2}$ to $2m_t$.

Fig. 7 shows that for $f=500$ GeV, as the coupling constant being near 0.0004, the result is close to the lower bound of the experimental data. While for $f=1000$ GeV, the prediction fits the experimental value when the coupling constant is above 0.0018.

Figure 8 shows that for $f=500$ GeV, taking the coupling constant within the range of 0.0003–0.0004, the result fits the experimental value. For $f=1000$ GeV, the prediction fits the experimental value when the coupling constant is above 0.0012. From the above analysis we have reached some conclusions. First, for $f=500$ GeV, the prediction can coincide with experimental data when the coupling constant takes a value of about 0.0003–0.0004. Second, for $f=1000$ GeV, the prediction could coincide with experimental data when the coupling constant takes a value between 0.0018–0.0028 and 0.0067–0.0087.

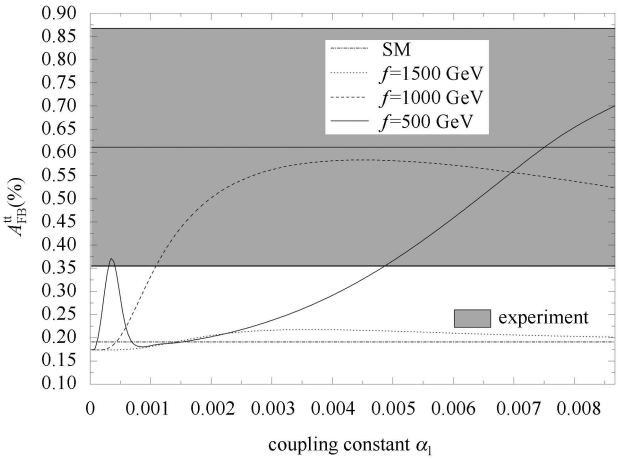

Fig. 8. The AFB with a cut of $|\triangle y|>1$ versus coupling constant in the frameworks of SM and LHM with $f=500$ GeV (solid), $f=1000$ GeV (dashed), $f=1500$ GeV (dotted). The dash-dotted line stands for the values from SM [13], and the shadowed region is for experimental data [10]. The uncertainty range is $\pm 3\%$ for μ in $\alpha_s(\mu)$ varies from $\frac{m_t}{2}$ to $2m_t$.

5 Discussion and conclusion

In this work, we study the contribution of LHM to the top quark forward backward asymmetry measured at Tevatron. With the help of the software LoopTools, we calculate the tree diagrams, box diagrams and their interference with the SM contributions. We find that only the Z_H boson in LHM makes a sizable contribution to the asymmetry when f runs from 500 GeV to 1000 GeV. As is understood, the new physics contribution should not significantly change the total cross section of the $t\bar{t}$ production, therefore there exists a small parameter space, which can reproduce the Tevatron asymmetry. When $f=500$ GeV, we predict that Z_H boson should be of a mass around 450 GeV. While for $f=1000$ GeV, the mass of Z_H boson is in two separate regions of 650–660 GeV and 750–850 GeV, respectively.

In recent years the LHC has been running, so we are able to analyze the effect of LHM on A_{FB}^{t} qualitatively. Since we know that the LHC is a p-p collider, the main process is $gg\to t\bar{t}$. The new gauge bosons in the LHM have no interaction with gluons. So they can only appear in one loop diagrams, thus A_{FB}^{t} have a $\frac{\alpha_s}{\pi}$ factor suppressed from the Tevatron.

It is said that a new state with a mass of about 500 GeV is probably excluded. So we hope that this viewpoint can be confirmed or denied in the lepton collider. For the expected ILC, whose center of mass energy is set to be 500 GeV in the early stage, we wish its center of mass energy to vary from 400 GeV to 500 GeV in order to find whether the $Z_{\rm H}$ boson with mass around 450 GeV indeed exists.

It is worth indicating that the D0 collaboration has updated their analysis on the lepton forward-backward asymmetry $A^{\rm l}_{\rm FB}$ [27] by including a measurement of an additional channel (lepton+3jets). Their new result of $A^{\rm l}_{\rm FB}$ is $4.2\pm2.4\%$ for $|y_{\rm l}|<1.5$, which is lower than the previous $15.2\pm4.0\%$ for $|y_{\rm l}|<1.5$ presented in Ref. [28]. Namely, the newly determined asymmetry $A^{\rm l}_{\rm FB}$ is reduced by 10.5% [27] as claimed by the collaboration. In Ref. [27] the authors explained the difference between the two analyses, in that in the previous analysis [28] only the channels (lepton+$\geqslant$4jets) are considered. In fact, most of the asymmetry in both the previous analysis [28] and current one [27] comes from lepton+$\geqslant$4jets channel with one b tag, meanwhile the lepton+3-jets channel makes a negative (opposite to the contribution of lepton+4-jets) contribution to the lepton forward-backward asymmetry to reduce the value of $A^{\rm l}_{\rm FB}$. Namely, the numerator of the asymmetry $A^{\rm l}_{\rm FB}$ decreases while the denominator slightly increases. Their re-analysis indicates that $A^{\rm l}_{\rm FB}$ is determined by the lepton+4-jets channel with one b tag is $16.3\pm4.8\%$ and its relative weight decreases from 50%, as given in Ref. [28], to 24%, as given in Ref. [27].

Even though the top quark forward-backward asymmetry needs a full reconstruction of the $\rm t\bar{t}$ decay chain [28], the asymmetry of top quark only concerns the on-shell top quark. Therefore, to evaluate the top asymmetry $A^{\rm t}_{\rm FB}$, we only need to include the part of $A^{\rm l}_{\rm FB}$ that comes from the on-shell top quark. The previous analysis on lepton forward-backward asymmetry includes only on shell top quarks, while in Ref. [27] the corresponding analysis of $A^{\rm l}_{\rm FB}$ contains contributions of both off-shell and on-shell top. In fact, the lepton+3 jets-events mainly come from off-shell top quark and, therefore, do not make a substantial contribution to $A^{\rm t}_{\rm FB}$. Thus, the new result given in Ref. [27] do not drastically change the experimental value of the top quark forward-backward asymmetry $A^{\rm t}_{\rm FB}$, thus our general conclusion does not change; that is, if one still uses the lepton+4-jets events to reconstruct the $\rm t\bar{t}$ production, then the original $A^{\rm l}_{\rm FB}\sim15.2\pm4.0\%$ would be unaffected and eventually the reconstructed $A^{\rm t}_{\rm FB}$ should remain unchanged, thus the allowed parameter space for LHM which we obtained would be the same as given in the text.

References

1 Aad G et al. (ATLAS collaboration). Phys. Lett. B, 2012, **717**: 330
2 Willenbrock S. Rev. Mod. Phys., 2000, **72**: 1141
3 Peters Y (D0 and CDF and ATLAS and CMS collaborations). arXiv:hepex/1112.0451
4 Bonciani R, Catani S, Mangano M L et al. Nucl. Phys. B, 1998, **529**: 424
5 Kidonakis N. Phys. Rev. D, 2010, **82**: 114030
6 Ahrens V, Ferroglia A, Neubert M et al. Phys. Lett. B, 2011, **703**: 135
7 Abazov V M et al. (D0 collaboration). Phys. Lett. B, 2009, **679**: 177
8 Aaltonen T et al. (CDF collaboration). Phys. Rev. D, 2010, **82**: 052002
9 Cheung K M, Keung W Y, YUAN T C. Phys. Lett. B, 2009, **682**: 287
10 Aaltonen T et al. (CDF collaboration). Phys. Rev. D, 2011,**83**: 112003
11 Aaltonen T et al. (CDF collaboration). CDF note, 2012, 108107
12 Abazov V M et al. (D0 Collaboration). Phys. Rev. D, 2011, **84**: 112005
13 Hollik W, Pagani D. Phys. Rev. D, 2011, **84**: 093003
14 CAO Q H, McKeen D, Rosner J L et al. Phys. Rev. D, 2010, **81**: 114004
15 SHU J, WANG K, ZHU G. Phys. Rev. D, 2012, **85**: 034008
16 Frampton P H, SHU J, WANG K. Phys. Lett. B, 2010, **683**: 294
17 Antunano O, Kuhn J H, Rodrigo G. Phys. Rev. D, 2008, **77**: 014003
18 Ferrario P, Rodrigo G. Phys. Rev. D, 2009, **80**: 051701
19 Aaltonen T T et al. (CDF collaboration). Phys. Rev. Lett, 2008, **101**: 202001
20 HAN T, Logan H E, McElrath B et al. Phys. Rev. D, 2003, **67**: 09500
21 Pumplin J, Stump D R, Huston J et al. JHEP, 2002, **0207**: 012
22 LI G, LI T, LI X Q et al. Nucl. Phys. B, 2005, **727**: 301
23 Eidelman S et al. Phys. Lett. B, 2004, **59**: 1
24 Fritzsch H, ZHOU Y. Phys. Rev. D, 2003, **68**: 034015
25 http://www-cdf.fnal.gov/physics/new/top/public_xsection.html
26 Kuhn J H, Rodrigo G. JHEP, 2012, **1201**: 063
27 Abazov V M et al. (D0 collaboration). arXiv:hepex/1403.1294
28 Abazov V M et al. (D0 collaboration). Phys. Rev. D, 2001, **84**: 112005